Int. J. Electrochem. Sci., 10 **(2015)** 4324 - 4334

International Journal of
ELECTROCHEMICAL
SCIENCE
www.electrochemsci.org

Electrochemical Behavior of Zirconium in an in-situ Preparing LiCl−KCl−$ZrCl_4$ Molten Slat

Yanqing Cai[1] , *Hongxia Liu*[1], *Qian Xu*[*,2], *Qiushi Song*[1], *Huijun Liu*[3], *Liang Xu*[1]

[1] School of Materials Science and Metallurgy, Northeastern University, Shenyang, 110004, PR China
[2] School of Materials Science and Engineering, Shanghai University, Shanghai, 200072, PR China
[3] Laboratory for Corrosion and Protection, Institute of Metal Research, Chinese Academy of Sciences, Shenyang, 110016, PR China
[*]E-mail: qianxu201@mail.neu.edu.cn

Received: 6 February 2015 / *Accepted:* 12 March 2015 / *Published:* 23 March 2015

The electrochemical behavior of zirconium was investigated in an in-situ preparing LiCl−KCl−$ZrCl_4$ molten slat at 773 K by cyclic voltammetry, chronopotentiometry, and open circuit chronopotentiometry. The concentration of $ZrCl_4$ in the salt is shown to have a great influence on the reduction process of zirconium. Two reduction steps at about −1.05 and −1.25 V due to Zr(IV)/Zr(II) and subsequently Zr(IV)/Zr and Zr(II)/Zr are observed at the lower concentration of $ZrCl_4$ (0.28 wt.%). At the medium concentration of $ZrCl_4$ (0.75 wt.% and 1.25 wt.%), another reduction step at −1.60 V corresponding to ZrCl/Zr is observed, indicating that Zr(IV) would reduce to ZrCl expecting for Zr at −1.25 V. What's more, the reduction of Zr(II) to ZrCl is also observed at −1.40 V at the higher concentration of $ZrCl_4$ (1.80 wt.%). In the anodic dissolution process, Zr firstly oxidizes to Zr(II) and Zr(IV), and then Zr(II) further oxidizes to Zr(IV).

Keywords: electrochemical behavior, zirconium, LiCl−KCl, cyclic voltammetry, chronopotentiometry

1. INTRODUCTION

Because of the low neutron capture cross section and good resistance to corrosion, zirconium becomes an irreplaceable component in the nuclear−power industry [1-3]. However, it must be nearly free of hafnium because hafnium absorbs neutrons very strongly [4]. Then the refining of zirconium has become one of the most challenges in the zirconium preparing for nuclear power industry. Molten salt electrorefining based on molten chloride or fluoride electrolyte has been developed as a promising option for effectively electrorefining or reprocessing the spent nuclear fuels or impurity metals [5-11].

Recently, a low-metling Zr-Cu-Sn alloy is proposed to be a liquid anode for electrorefining sponge Zr, and the purpose is to obtain high purity nuclear zirconium at the cathode [12]. For the introduction difficulty of $ZrCl_4$, which is hydrophilic and expensive, and usually sublimates at a low temperature (331℃) [2], we have in-situ prepared $ZrCl_4$ in LiCl−KCl molten salt by the replacement reaction between CuCl and Zr[13]. Then the reduzate Cu will return to the liquid anode without of introducing impurities, and the prepared LiCl−KCl−$ZrCl_4$ will be used as the electrolyte in the electrorefining of Zr. However, an electrode potential is necessary to preferentially separate zirconium from the alloys by depositing it on the cathode within the electrochemical cell. Thus, the precise information about reduction and oxidation potentials of zirconium in the prepared LiCl−KCl−$ZrCl_4$ melt is significant to improve the purity and process efficiency [14].

At present, several investigators have investigated the electrochemical behavior of zirconium in alkali chloride molten slat systems [8, 14-22], especially in the LiCl−KCl molten slat containing $ZrCl_4$. Basile et al.[17] have reported that the electrodeposition of zirconium in a LiCl−KCl eutectic containing $ZrCl_4$ is a two-step process, and Zr(IV) firstly reduces to $ZrCl_2$ and follows by the reduction of $ZrCl_2$ to Zr. He did not find the existence of ZrCl, and insisted that $ZrCl_2$ is an insoluble compound. Sakamura[22] found that Zr(IV) reduces to ZrCl and Zr at the cathode, and ZrCl and $ZrCl_2$ are metastable compounds and would slowly disproportionate into Zr(IV) and Zr. At the anode, Zr and ZrCl are dissolved into the melt as Zr(IV). Ghosh et al.[23, 24] have reported the redox behavior of zirconium in LiCl−KCl melt with the absence and presence of Zr metal. The simultaneous reduction peaks of Zr^{4+}/Zr^{2+}, Zr^{2+}/Zr and Zr^{2+}/Zr^{+} appear in the absence of Zr, while Zr^{4+}/Zr^{2+} disappears in the presence of Zr. Lee[19] and Park[8] have also investigated the zirconium behavior in LiCl−KCl melt with 4.0 wt.% and 1.0 wt.% $ZrCl_4$ on the tungsten electrode, respectively. Both of them agreed that Zr(IV) continuously reduces to Zr(II), ZrCl and Zr during the reduction process. The difference is that Lee considered Zr(II) directly reduces to Zr while Park insisted Zr(II) firstly reduces to ZrCl and then to Zr.

In summary, due to the complex electrochemical behavior of zirconium which consists of a series of stepwise processes and the low sublimation point of $ZrCl_4$ [25], there exists large disagreements among the studies with regard to the reduction mechanism of Zr(IV). What's more, most of the studies are only conducted at a single concentration of $ZrCl_4$, which is directly introduced into the salt. Hence, in the present study, a detailed electrochemical study of zirconium was conducted in an in-situ preparing LiCl−KCl−$ZrCl_4$ melt with the replacement reaction of Zr metal and CuCl. What's more, the redox process of zirconium was investigated at various concentrations of $ZrCl_4$ by a series of electrochemical techniques, such as cyclic voltammetry, chronopotentiometry, and open circuit chronopotentiometry. Additionally, the potentiostatic deposits were also characterized by XRD analysis.

2. EXPERIMENTAL

A three-electrode cell was assembled in an alumina crucible placed in a stainless steel reactor in a vertical tube furnace, as shown in Fig. 1 [13]. All the experiments were conducted under an inert

argon atmosphere. The temperature was maintained at 773 K measured using a chromel-alumel thermocouple with an accuracy of ±2 K. Molybdenum wire (Ø1 mm, 99.95% purity) and zirconium wire (Ø3 mm, 99.4% purity) were used as working electrodes (WE) for the investigation of electrochemical behaviors. The counter electrode (CE) was a graphite rod (Ø10 mm, spectrum pure), which provided by the Shanghai new graphite material Co., Ltd. of Sinosteel Corporation (Shanghai, China). The electrode surface area was determined by measuring the immersion depth of the electrode in the molten salt after each experiment. The reference electrode (RE) was LiCl−KCl−1.0 wt.% AgCl melt contained in a closedend mullite tube with a silver wire (Ø1 mm, 99.99% purity) immersed into it for electrical connections. In this paper, all potentials are referred to this electrode.

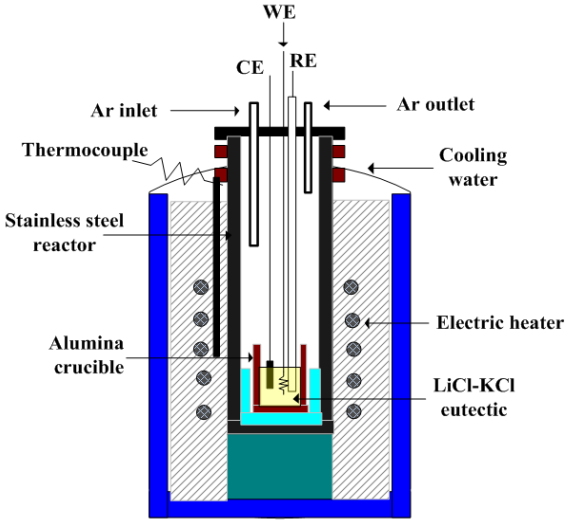

Figure 1. Schematic diagram of experimental apparatus [13]

An analytical grade anhydrous LiCl−KCl (58.5:41.5 mol.%) mixture, previously dehydrated under 573 K for at least 24 h, was served as the base electrolyte. Copper (I) was introduced into the bath in the form of analytical grade anhydrous CuCl powder for the replacement reaction. LiCl−KCl−$ZrCl_4$ melt was prepared by taking stoichiometric amount of CuCl and zirconium rods (Ø3 mm×20 mm, 99.5% purity) in excess and equilibrating them in molten LiCl−KCl melt inside an argon atmosphere for 3 h at 773 K. The concentration of $ZrCl_4$ was changed by the adding amount of CuCl, and was finally determined by an inductively coupled plasma−atomic emission spectrometer (ICP−AES). The cathode deposits were identified by an X-ray diffractometer (XRD).

All electrochemical studies were performed with AUTOLAB/PGSTAT320 potentiostat/ galvanostat from M/s. EcoChemie, Netherlands, and the data acquisition was controlled by GPES 4.9 software for cyclic voltammetry, chronopotentiometry and open circuit chronopotentiometry.

3. RESULTS AND DISCUSSION

3.1 Cyclic voltammetry on Mo electrode at various Zr(IV) concentrations

Cyclic voltammograms (CVs) measurements were carried out on inert Mo electrodes at 773 K. Fig. 2(a-d) shows a set of CVs obtained from LiCl−KCl eutectic with various concentrations of $ZrCl_4$,

which are 0.28 wt.%, 0.75 wt.%, 1.25 wt.%, and 1.80 wt.%, respectively. At the medium concentration of $ZrCl_4$ (0.75 wt.% and 1.25 wt.%), as shown from Fig. 2(b) and Fig. 2(c), two couples of C/C' and E/E' are both observed at potential range from −0.8 to −1.3 V. What's more, cathodic peak D' and anodic peak D are also obtained. The couple E/E' should correspond to the redox couple of Zr(IV)/Zr(II), and peak C' is mainly attributed to the reduction of Zr(IV) to Zr and ZrCl, and Zr(II) to Zr. What's more, anodic peak D, which appears by varying the scan range to peak C', should correspond to the oxidation of ZrCl to Zr(IV). It disappears after the potential scans to peak D', which is related to the reduction of ZrCl to Zr. Then anodic peaks C and E are only remained, which are related to the oxidation of Zr to Zr(II) and Zr(IV), and Zr(II) to Zr(IV), respectively. Since the peak E and E' had relatively smaller height than other peaks, they are less conspicuous in Fig. 2. These results obtained at the medium concentration of $ZrCl_4$ (0.75 wt.% and 1.25 wt.%) are similar with those reported by the literatures [14, 17, 19, 22], which were all conducted in a signal concentration of $ZrCl_4$ (about 1.0 wt.%).

Peak E': $Zr(IV) + 2e \rightarrow Zr(II)$ (1)

Peak C': $Zr(IV) + 4e \rightarrow Zr$ (2)

$Zr(IV) + 3e + Cl^- \rightarrow ZrCl$ (3)

$Zr(II) + 2e \rightarrow Zr$ (4)

Peak D': $ZrCl + e \rightarrow Zr + Cl^-$ (5)

Peak F': $Zr(II) + e + Cl^- \rightarrow ZrCl$ (6)

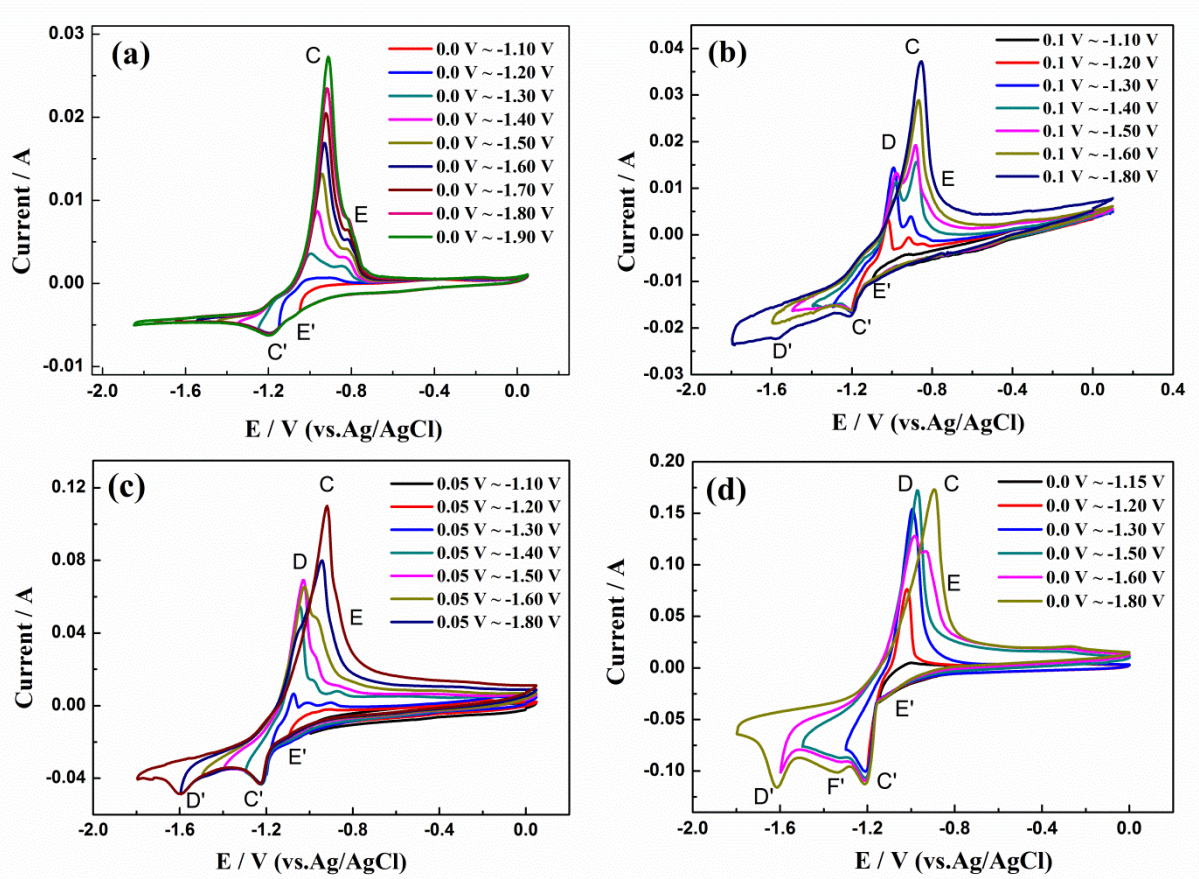

Figure 2. CVs on molybdenum electrode in LiCl−KCl eutectic with (a) 0.28 wt.%, (b) 0.75 wt.%, (c)1.25 wt.%, and (d)1.80 wt.% $ZrCl_4$ dissolving in the molten salt. Apparent electrode area: 0.628 cm^2, scan rate: 100 mV s^{-1}.

Peak C: $Zr - 4e \rightarrow Zr(IV)$ (7)

$Zr - 2e \rightarrow Zr(II)$ (8)

Peak E: $Zr(II) - 2e \rightarrow Zr(IV)$ (9)

Peak D: $ZrCl - 3e \rightarrow Zr(IV) + Cl^-$ (10)

However, in the present study, there are some different opinions about the reduction mechanism of Zr(IV) at different concentrations of $ZrCl_4$, which has never been reported. At the low concentration of Zr(IV), as shown in Fig. 2(a), anodic peak D are not obtained when the cathodic potential scans to peak C'. Subsequently, the cathodic peak D' is not observed. It indicates that the reduction of Zr(IV) to ZrCl at peak C' is impossible at a low Zr(IV) concentration. On the other hand, with the increase of Zr(IV) concentration, the peak current of D appears and increases gradually when the potential scans to −1.40 V as shown in Fig. 2(b-d), while the peak current of C declines and disappears at the same time. Correspondingly, the reduction peak of D' appears and becomes more defined as the expansion of scan range to −1.80 V. The possible reason is that there may exist a competition between the reduction of Zr(IV) to Zr and ZrCl. At a low Zr(IV) concentration (0.28wt.%), Zr(IV) is preferentially reduced to Zr metal instead of ZrCl. While at a high Zr(IV) concentration(1.80 wt.%), Zr(IV) is more conducive to reducing to ZrCl. Thus the oxidation peak D and the reduction peak D' increase obviously with the increasing Zr(IV) concentration. What's more, at the high concentration of Zr(IV), as shown in Fig. 2(d), a cathodic peak F' is also observed, which has never been reported. With the scan range shifting from −1.30 to −1.50 V, the redox peak of D increases, indicating that peak F' might correspond to the reduction of Zr(II) to ZrCl. The speculation has been proved by the XRD results.

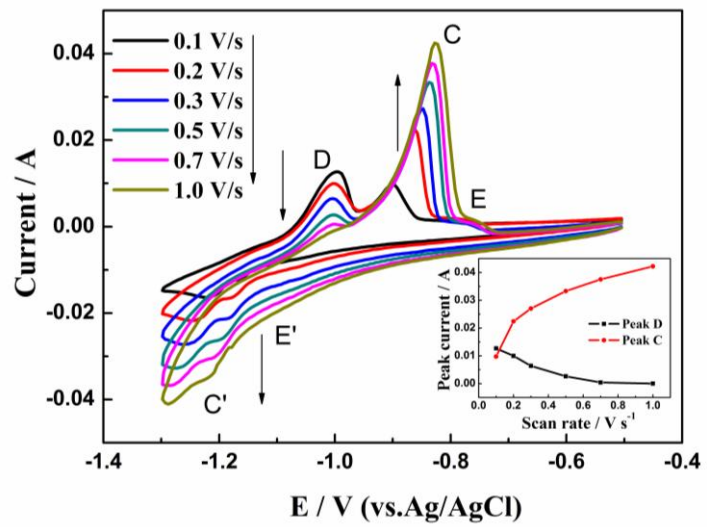

Figure 3. CVs of the LiCl−KCl−0.75 wt.% $ZrCl_4$ with various scan rates on molybdenum electrode at 773 K. The inset shows the relationship between the anodic peak currents of D and C and scan rate. Apparent electrode area: 0.628 cm^2.

Fig. 3 shows a set of CVs obtained in LiCl−KCl−0.75wt.% $ZrCl_4$ melt over a potential range from −1.30 to −0.30 V while changing scan rate from 0.1 to 1.0 V/s. The inset shows the relationship between the anodic peak currents of D and C and scan rate. At the lower scan rate of 0.1 V/s, the peak

current of D is a little higher than peak C, and both of them are noticeable. However, the peak current of D begins to decline with the increase of the scan rate, and is hard to be detected at 1.0 V/s. While the peak current of C increases as the rise of the scan rate, and the potential of peak C shifts about 75 mV toward a positive direction. As shown from the inset of Fig.3, it is concluded that Zr(IV) reduces to ZrCl and Zr at −1.20 V at a low scan rate, then the reduction reaction of Zr(IV) to ZrCl becomes weaker as the increase of scan rate, while to Zr strengthens. In other words, cathodic peak C' is attributed to reaction (3) only when the scan rate is low. Sakamura [22] has also mentioned these changes, but he did not report the relationship between the peak currents of D and C and scan rate detailedly. Above all, Zr(IV) would be reduced to ZrCl only when the Zr(IV) concentration is high and the scan rate is low.

3.2 Cyclic voltammetry on Zr electrode

To further explore the electrochemical behavior of zirconium, cyclic voltammetry was performed on a Zr working electrode. Fig. 4 presents a set of CVs obtained in the LiCl−KCl−1.80 wt.% $ZrCl_4$ melt with various starting potentials at a fixed scan rate of 100 mV/s. In the beginning, as shown in Fig. 4(a), the anodic peaks C and E are observed when the starting potentials are −1.0 and −1.1 V, respectively. Afterwards, with the starting potential shifting negatively, anodic peak D is observed with the potential scanning to cathodic peak C'. It indicates that Zr would oxidize into Zr(IV) directly and no peaks about the oxidation of ZrCl appear firstly. When the potential shifting to −1.2 V, the reduction of Zr(IV) to ZrCl happens at peak C', and correspondingly, the oxidation of ZrCl to Zr(IV) is obtained at peak D. With the potential continually shifting negatively, as shown in Fig. 4(b), cathodic peaks F' and D' are observed. However, anodic peak D begins to decline with the potential shifting to −1.7 V, which causes by the reduction of ZrCl to Zr at peak D'. The results obtained at Zr electrode are well consistent with those obtained at Mo electrode in the LiCl−KCl−$ZrCl_4$ melt.

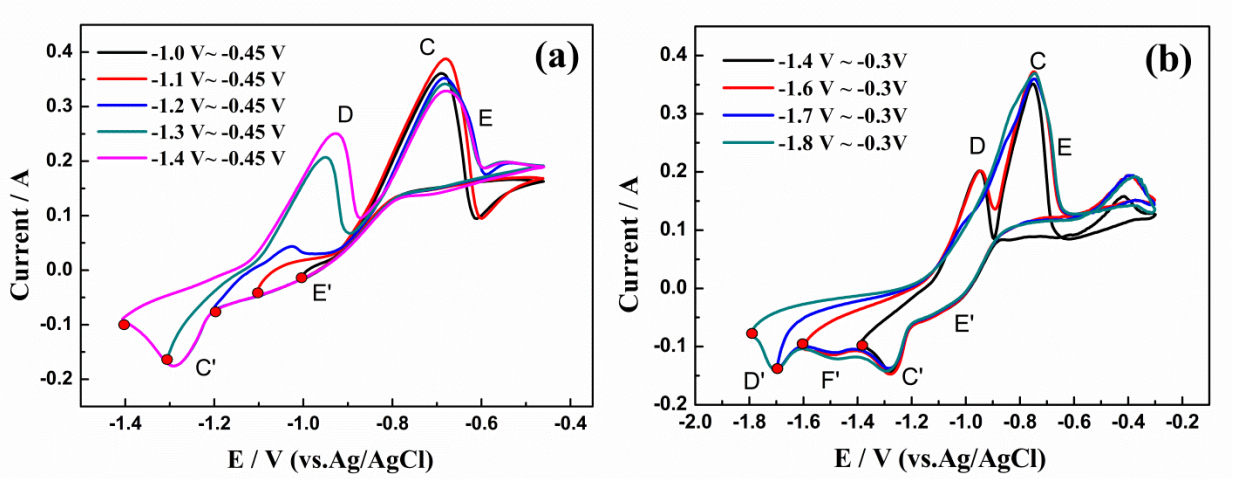

Figure 4. CVs of the LiCl−KCl−1.80 wt.% $ZrCl_4$ melt with various starting scan potentials on zirconium electrode at 773 K. Apparent electrode area: 1.256 cm^2, scan rate: 100 mV s^{-1}.

3.3 Chronopotentiometry

To further confirm the reduction mechanism of Zr(IV), chronopotentiometry was also carried out in LiCl−KCl melt at different current densities. Fig. 5 shows the chronopotentiograms obtained with various Zr(IV) concentrations for a Mo electrode. At a lower concentration of $ZrCl_4$ (0.28 wt.%), as shown in Fig. 5(a), plateau τ_1 is observed at about −1.0 V, which is interpreted as the reduction of Zr(IV) to Zr(II). After that, plateau τ_2 at −1.25 V is correlated with the reduction of Zr(IV) and Zr(II) to Zr. Finally, plateau τ_0 at about −2.40 V corresponds to the reduction of Li^+ to metallic Li. At the medium concentration of $ZrCl_4$ (1.25 wt.%), as shown in Fig. 5(b), apart from the plateaus obtained in Fig. 5(a), the chronopotentiograms consist of one new plateau τ_3 at −1.60 V, which is related to the reduction of ZrCl to Zr. What's more, expecting for the reduction of Zr(IV) and Zr(II) to Zr, plateau τ_2 should also present the reduction of Zr(IV) to ZrCl. Fig. 5(c) shows the chronopotentiograms obtained in the LiCl−KCl melt containing 1.80 wt.% $ZrCl_4$. It is in particularly noteworthy that between the plateaus τ_2 and τ_3, plateau τ_4 at about −1.40 V is observed, which may be due to the reduction of Zr(II) to ZrCl. The plateaus τ_1 and τ_2 obtained here are similar to the results reported by Ghosh et. al [24], who has investigated the chronopotentiograms in LiCl−KCl−2.1wt.% $ZrCl_4$ molten salt on a tungsten. However, the disagreement is that plateaus τ_3 and τ_4 were not mentioned by Ghosh et. al, although an obvious plateau at −1.60 V is observed. It is obvious that all potential plateaus obtained by chronopotentiometry in Fig. 5 are completely coincided with the cathodic peaks obtained in the CVs results.

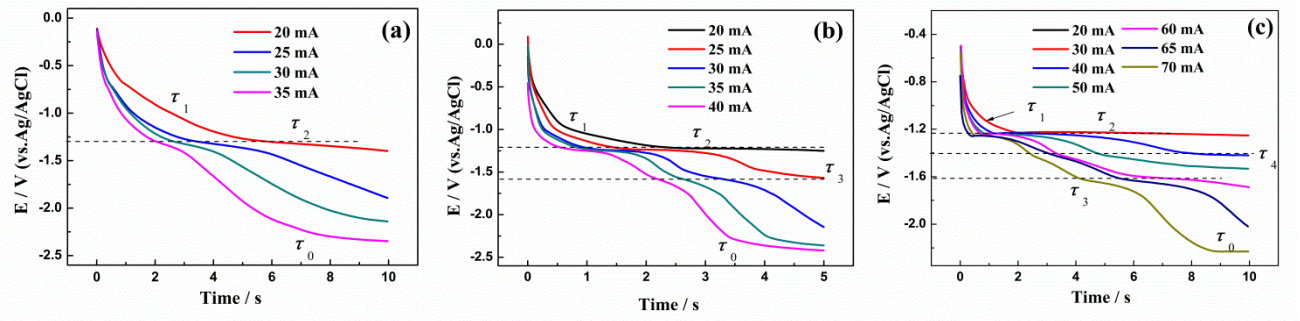

Figure 5. Chronopotentiograms in LiCl−KCl with (a) 0.28 wt.%, (b) 1.25 wt.%, and (c) 1.80 wt.% $ZrCl_4$ dissolving in the molten salt at different current densities for a Mo electrode. Apparent electrode area: 0.628 cm^2.

3.4 Open circuit chronopotentiometry

Open circuit chronopotentiometry was also performed to study the formation and dissolution of zirconium by depositing a thin layer of metals on molybdenum electrode for a short period. The open−circuit potential of the electrode was registered as a function of time after switching off the potentiostatic control. The potential plateaus corresponded to biphasic equilibrium of coexisting state at the electrode surface would be observed[26, 27].

Fig. 6 presents an open circuit chronopotentiogram obtained in LiCl−KCl−1.25 wt. % $ZrCl_4$ melt after electrodepositing at −2.60 V vs. Ag/AgCl for 10 s on molybdenum electrode at 773 K.

Firstly, the potential maintains at a potential close to −2.40 V (plateau a), which is related to the Li^+/Li equilibrium potential. Afterwards, plateau b at around −1.02 V is corresponded to the deposition of Zr and associated with the Zr(IV)/Zr and Zr(II)/Zr redox couples. Apart from these two identified potential plateaus (a, b), plateau c is observed at −0.88 V, which is less conspicuous as the same in the CV results. It should correspond to the equilibrium potential of Zr(IV)/Zr(II) couple. The present results from open circuit chronopotentiometry are in agreement with those of Ghosh et. al [24], and they clearly show the dissolution of Zr and are well consistent with the oxidation process in the cyclic voltammetry.

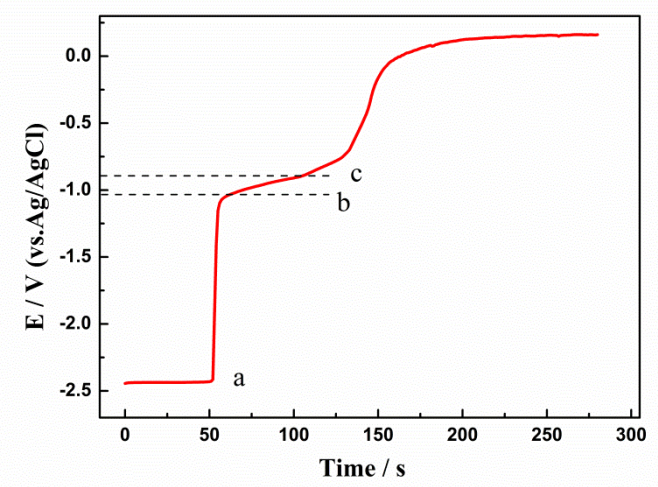

Figure 6. OCP of LiCl−KCl−1.25 wt. % $ZrCl_4$ melt after electrodepositing at −2.60 V vs. Ag/AgCl for 10 s on molybdenum electrode at 773 K. Apparent electrode area: 0.628 cm^2.

3.5 Characterization of the cathodic deposits

An electrodeposition test was carried out to identify the zirconium deposits versus the cathode potentials, which were previously defined by cyclic voltammetry and chronopotentiometry. As shown from the electrochemical tests, Zr(IV) would directly reduce to zirconium with a low concentration of $ZrCl_4$, which could improve the current efficiency in the refining process. However, the electrorefining time would be seriously prolonged. It could not be applied in the actual operation. Then electro-deposits are prepared in the LiCl−KCl−1.80 wt.% $ZrCl_4$ melt on a molybdenum electrode with an alumina catch crucible (o.d. 10 mm) placed under the wire cathode to recover the deposit falling from the wire. The constant potentials of −1.25, −1.40, and −1.60 V, where the reduction peaks (C', F', D') appear on cyclic voltammetry and plateaus (τ_2, τ_3, τ_4) on chronopotentiometry, are applied on the molybdenum electrode for more than an hour as shown in the current transient of Fig. 7(a). The reduction currents gradually increase over time due to an expansion of the surface area [22]. After electrolysis, the deposits are taken out from the salt and prepared for the XRD analysis by dissolving the salts in deionized water and following by air drying at room temperature. They look different from the color, which are respectively gray, nigger-brown and black powders with the potentials shifting negatively. Fig. 7(b) presents the XRD patterns of zirconium compounds deposited at −1.25, −1.40, and −1.60 V, respectively. For the zirconium compounds obtained at −1.25 V, the major peaks are

related to be ZrCl, $Zr_{1.05}Cl_2$, ZrO_2, and also with some Zr. Among them, the appearance of ZrCl and $Zr_{1.05}Cl_2$ indicates that some zirconium chlorides with intermediate valence (+1, +2) might be insoluble or have a low solubility. ZrO_2 is also found which may because of the oxidization and hydrolyzation of the insoluble zirconium chlorides[28]. When the applied potential is −1.40 V, the mainly peaks are corresponded to ZrO_2, ZrCl and Zr. Observably, $Zr_{1.05}Cl_2$ disappears, which interprets that Zr(II) has reduced to ZrCl at −1.40 V. Additionally, the peaks of metallic Zr obtained at −1.25 and −1.40 V are very low, while ZrCl and $Zr_{1.05}Cl_2$ are the mainly products, which indicates that Zr(IV) mainly reduces to Zr(II) and Zr(I) at this potential range. Moreover, the XRD patterns for the products obtained at −1.60 V are only associated with Zr metal, indicating that all the zirconium chlorides have been reduced to metallic zirconium. Similar electrodeposition tests were previously carried out by Iizuka [29] and Sakamura [22]. Iizuka found that only ZrCl in the cathode deposits, while Sakamura discovered the existence of Zr. Both of them did not find the existence of $Zr_{1.05}Cl_2$. It is possible because that part of Zr(II) chloride might have a low solubility and forms $Zr_{1.05}Cl_2$ with ZrCl. The XRD results well confirm the state of products obtained at the potentials of −1.25, −1.40, and −1.60 V, which are in good agreement with the electrochemical analyses. What's more, the observations provide a basis for the electrorefining of Zr from the in-situ preparing LiCl−KCl−$ZrCl_4$ melt in the future.

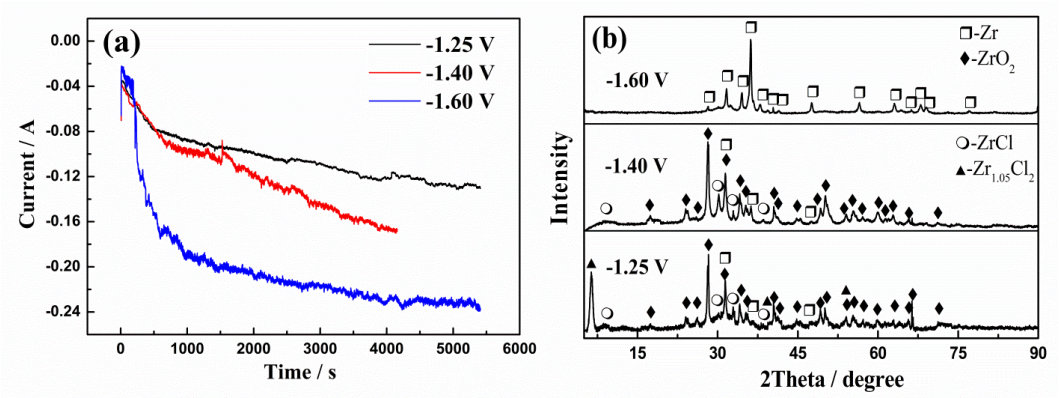

Figure 7. (a) Current transients for Zr reduction, and (b) XRD patterns of the cathode deposits obtained in LiCl−KCl−1.80 wt.% $ZrCl_4$ molten salt at potentials of −1.25 V, −1.40 V and −1.60 V, respectively. Apparent electrode area: 0.628 cm^2.

4. CONCLUSIONS

The electrochemical behavior of $ZrCl_4$ was investigated in an in-situ prepared LiCl−KCl−$ZrCl_4$ molten salt by the replacement reaction between Zr and CuCl at 773 K. By conducting a series of electrochemical techniques, such as cyclic voltammetry and chronopotentiometry, the reduction process of Zr(IV) to Zr was investigated with different concentration of $ZrCl_4$. The results show that Zr(IV) is firstly reduced to Zr(II) and then with simultaneous reduction of Zr(IV) to Zr and Zr(II) to Zr at the lower concentration of $ZrCl_4$ (0.28 wt.%). While at the medium concentration of $ZrCl_4$ (0.75 wt.% and 1.25 wt.%), a reduction step due to ZrCl/Zr is observed at −1.60 V, which indicates that Zr(IV) would first reduce to ZrCl at the positive potential of −1.25 V. With the concentration of $ZrCl_4$

increasing to 1.80 wt.%, the reduction of Zr(II) to ZrCl at −1.40 V is also observed. Based on the XRD analysis, insoluble zirconium chlorides with intermediate valence (+1, +2) might exist in the intermediate reduction process. When the potential is applied at −1.60 V, pure zirconium is obtained. Moreover, Zr is directly oxidizes to Zr(II) and Zr(IV), then Zr(II) further oxidizes to Zr(IV) during the anodic dissolution process. The investigation on the electrochemical behavior of zirconium will provide a basis for the electrorefining of Zr from the in-situ preparing LiCl−KCl−$ZrCl_4$ melt with a liquid Cu-Sn-Zr anode in the future.

ACKNOWLEDGEMENTS
The authors acknowledge the financial support of National Natural Science Foundation of China (Grant No. 51174055).

References

1. D. L. Douglass, *Metallurgy of zirconium*, Univ. of California, Los Angeles, (1971).
2. W. J. Kroll and F. E. Bacon, US Patent 2, 443, 253, (1948).
3. W. Kroll, A. Schlechten, W. Carmody, L. Yerkes, H. Holmes and H. Gilbert, *T. Electrochem. Soc.*, 92 (1947) 99.
4. T. Murakami and T. Kato, *J. Electrochem. Soc.*, 155 (2008) E90.
5. T. Murakami, Y. Sakamura, N. Akiyama, S. Kitawaki, A. Nakayoshi and M. Fukushima, *J. Nucl. Mater.*, 414 (2011) 194.
6. M. Iizuka, T. Omori and T. Tsukada, *J. Nucl. Sci Technol.*, 47 (2010) 244.
7. C. Hwa Lee, Y. L. Lee, M. K. Jeon, Y. T. Choi, K. H. Kang and G. I. Park, *J. Nucl. Mater.*, 449 (2014) 93.
8. K. T. Park, T. H. Lee, N. C. Jo, H. H. Nersisyan, B. S. Chun, H. H. Lee and J. H. Lee, *J. Nucl. Mater.*, 436 (2013) 130-138.
9. K. Kinoshita, T. Koyama, T. Inoue, M. Ougier and J.-P. Glatz, *J. Phys. Chem. Solids*, 66 (2005) 619.
10. Y. Jung, *Int. J. Electrochem. Sci.*, 8 (2013) 6784.
11. T. J. Kim, D. H. Ahn, S. W. Paek and Y. Jung, *Int. J. Electrochem. Sci.*, 8 (2013) 9180.
12. Y. Xiao, A.V. Sandwijk, Y. Yang, V. Laging, *Molt. Salts. Chem. Technol.*, (2014) 389.
13. Y. Q. Cai, H. X. Liu, Q. Xu, Q. S. Song, L. Xu, *Elctrochim. Acta*, 161 (2015) 177.
14. J. Park, S. Choi, S. Sohn, K. Kim and I. S. Hwang, *J. Electrochem. Soc.*, 161 (2014) H97.
15. Y. Wu, Z. Xu, S. Chen, L. Wang and G. Li, *Rare Metals*, 30 (2011) 8.
16. Z. Chen, Y. J. Li and S. J. Li, *J. Alloy Compd.*, 509 (2011) 5958.
17. F. Basile, E. Chassaing and G. Lorthioir, *J. Appl. Electrochem.*, 11 (1981) 645.
18. C. Guang-Sen, M. Okido and T. Oki, *J. Appl. Electrochem.*, 20 (1990) 77.
19. C. H. Lee, K. H. Kang, M. K. Jeon, C. M. Heo and Y. L. Lee, *J. Electrochem. Soc.*, 159 (2012) D463.
20. G. Kipouros and S. Flengas, *J. Electrochem. Soc.*, 132 (1985) 1087.
21. P. Pint and S. Flengas, (1976).
22. Y. Sakamura, *J. Electrochem. Soc.*, 151 (2004) C187.
23. S. Ghosh, S. Vandarkuzhali, N. Gogoi, P. Venkatesh, G. Seenivasan, B. P. Reddy and K. Nagarajan, *Elctrochim. Acta*, 56 (2011) 8204.
24. S. Ghosh, S. Vandarkuzhali, P. Venkatesh, G. Seenivasan, T. Subramanian, B. Prabhakara Reddy and K. Nagarajan, *J. Electroanal. Chem.*, 627 (2009) 15.
25. C. P. Fabian, V. Luca, T. H. Le, A. M. Bond, P. Chamelot, L. Massot, C. Caravaca, T. L. Hanley and G. R. Lumpkin, *J. Electrochem. Soc.*, 160 (2012) H81.

26. Y. D. Yan, H. Tang, M. L. Zhang, Y. Xue, W. Han, D. X. Cao and Z. J. Zhang, *Elctrochim. Acta*, 59 (2012) 531.
27. H. Tang, Y. D. Yan, M. L. Zhang, X. Li, Y. Huang, Y. L. Xu, Y. Xue, W. Han and Z. J. Zhang, *Elctrochim. Acta*, 88 (2013) 457.
28. Y. X. Huang, C. J. Guo, *J. Inorg. Mater.*, 7 (1992)483.
29. M. Iizuka, CRIEPI Report (in Japanese), (1998) T98001.